Macromolecules

ARTICLE

pubs.acs.org/Macromolecules

One-Step Functionalization of Single-Walled Carbon Nanotubes (SWCNTs) with Cyclopentadienyl-Capped Macromolecules via Diels–Alder Chemistry

Nicolas Zydziak,[†,‡] Christof Hübner,[‡] Michael Bruns,[§] and Christopher Barner-Kowollik*[,†]

[†]Preparative Macromolecular Chemistry, Institut für Technische Chemie und Polymerchemie, Karlsruhe Institute of Technology (KIT), Engesserstrasse 18, 76128 Karlsruhe, Germany

[‡]Polymer Engineering Department, Fraunhofer Institute of Chemical Technology, Joseph-von-Fraunhofer-Str. 7, 76327 Pfinztal, Germany

[§]Institute for Materials Research III and Karlsruhe Nano Micro Facility (KNMF), Karlsruhe Institute of Technology (KIT), Hermann-von-Helmholz-Platz 1, 76344 Eggenstein-Leopoldshafen, Germany

Supporting Information

ABSTRACT: Without previous modification, single-walled carbon nanotubes (SWCNTs) react as dienophiles in a single-step Diels–Alder [4 + 2] cycloaddition with diene terminal polymer strands. Cyclopentadienyl-capped poly(methyl methacrylate) (M_n = 2900 g mol^{-1}, PDI = 1.2) was grafted onto SWCNTs under mild conditions at ambient temperature as well as at 80 °C in the absence of any catalyst. Thermogravimetric analysis, elemental analysis, and X-ray photoelectron spectroscopy confirm the success of the reaction and allow to estimate the grafting density of the polymer chains on the SWCNTs via the above three independent methods (average grafting density of 0.064 mmol g^{-1} (0.029 chains nm^{-2}) for samples reacted at ambient temperature and 0.086 mmol g^{-1} (0.039 chains nm^{-2}) for samples reacted at 80 °C). In addition, high-resolution transmission electron microscopy images confirmed the presence of an amorphous polymer layer (~3 nm) around the SWCNTs after functionalization.

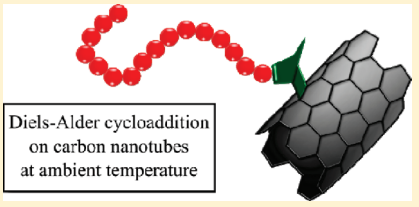

INTRODUCTION

Carbon nanotubes (CNTs) are highly interesting entities as they can reinforce existing polymeric materials[1−3] as well as induce electrical conductivity into the polymer.[1,4−6] However, to achieve an efficient and uniform distribution of the CNTs in a given polymeric material, a suitable functionalization of the CNTs is required. Generally, when CNTs are intermixed with the polymeric material, phase separation and bundling are often observed,[7,8] leading to little or no physically desired effects from the presence of the CNTs in the polymeric compound.[9,10] Thus, efficient and facile strategies are required for a covalent modification of CNTs with suitable polymer strands and for good embedding of the CNTs into the polymer matrix. Ideally, one would envisage a functionalization process that requires no prior treatment of the employed CNTs as well as leaving the CNT's structure as much as possible intact. In the past, several strategies for the covalent functionalization of CNTs have been suggested. These strategies are described in several reviews[6,11−13] and include, among others, oxidation,[14,15] fluorination,[16] free radical addition,[17] addition of carbenes and nitrenes,[18] 1,3 dipolar cycloaddition,[19] Bingel reaction,[20] nucleophilic addition,[21] and alkylation.[22] All these strategies require relatively demanding reaction conditions as the chemicals involved can be highly sensitive to atmospheric exposure (moisture, air), and several synthetic steps are required in order to functionalize the CNTs. We submit, however, that Diels–Alder [4 + 2] cycloadditions may indeed be conducted onto the single-walled carbon nanotubes' (SWCNTs) surface with judiciously selected polymer precursors under very mild conditions, leading to a rapid and selective functionalization as well as high conversions.[23]

Recently, the functionalization of fullerenes with single polymer chains via a direct and rapid ambient temperature reaction between neat fullerenes and cyclopentadiene functional polymer chains was demonstrated by our research group.[24] The functionalization of fullerenes (C_{60}) with macromolecular building blocks is an interdisciplinary research area,[25] combining the unique electronic and optical properties of fullerenes with the highly variable physiochemical properties of polymeric materials. The cyclopentadienyl functionalization concept can be transferred to SWCNTs and contribute to define a simplified and innovative way for introducing SWCNTs into polymer matrices and increasing the performance and efficiency of e.g. photovoltaic devices.[26] Driven by our success in the direct and catalyst-free [4 + 2] fullerene functionalization with polymer strands, in the current contribution we apply a Diels–Alder functionalization strategy for the direct (ambient temperature) covalent

Received: January 16, 2011
Revised: February 26, 2011
Published: April 07, 2011

Scheme 1. Synthetic Pathway for the Direct [4 + 2] Functionalization of Single-Walled Carbon Nanotubes (SWCNTs) with Cyclopentadiene-Capped Poly(methyl methacrylate)

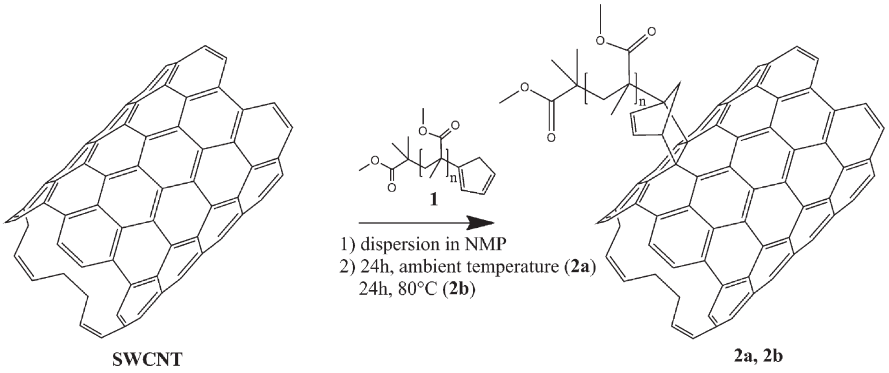

functionalization of SWCNTs. Such a functionalization strategy fulfils the criterion of requiring no premodification of the CNTs and thus opens the possibility of being applied in a single process step when modifying a polymer matrix with functional CNTs. The possibility of CNTs to react in Diels−Alder reaction as dienes or dienophiles has been discussed since 2002[27−29] and confirmed by experimental data, although the synthetic pathways remained relatively demanding. The work performed by Ménard-Moyon et al. involves the use of metal complexes $Cr(CO)_6$ under high pressure (1.3 GPa).[30] In an alternative approach, the thermal degradability of furfuryl alcohols requires the total absence of oxygen as reported by Munirasu et al.[31] In addition, a Diels−Alder reaction to conjugate CNTs with a polymer functioning as diene was conducted by Hadjichristidis and colleagues at high temperature (close to 200 °C) to afford cross-linked structures of phenylbenzylcyclobuteneethylene with multiwalled carbon nanotubes.[32] The proposed route in the present contribution enables the functionalization of SWCNTs in a one-pot reaction under mild conditions. Our approach is based on the high reactivity of cyclopentadienyl-capped polymers (dienes) to undergo reactions with SWCNTs (dienophiles) at ambient temperature as well as higher temperature (80 °C) in air in the absence of any catalyst. The employed synthetic pathway is depicted in Scheme 1.

Evidencing the success of the functionalization reaction is not as straightforward as in the case of functional fullerenes, as the polymer-functionalized SWCNTs do not spontaneously dissolve in any solvent system and thus cannot be analyzed via e.g. soft ionization mass spectrometric techniques.[33] The characterization approach taken in the current study combines quantitative (surface analysis) methods to prove the successful [4 + 2] cycloaddition of cyclopentadiene-capped polymers onto the SWCNTs. Thermogravimetric analysis (TGA) was conducted to observe changes in the thermal response profiles and to estimate the grafting density of polymer chains attached onto the SWCNTs. Complementary to TGA, elemental analysis (EA) and X-ray photoelectron spectroscopy (XPS) enable the determination of the elemental composition (throughout the bulk and the surface) of the sample and enable the comparison of the grafting density estimated via these three methods. In addition, high-resolution transmission electron microscopy (HRTEM) was performed to illustrate the modified surface of the SWCNTs after the [4 + 2] cycloaddition and to deduce the thickness of the grafted polymer layer. Poly(methyl methacrylate) was chosen as it can be readily prepared with a preselected chain length and narrow polydispersity via atom transfer radical polymerization (ATRP), featuring a bromine chain terminus, which is readily switchable to a highly [4 + 2] active cyclopentadiene (Cp) entity in a quantitative fashion as recently demonstrated by us.[34] Most importantly, poly(methyl methacrylate) contains oxygen atoms which can be readily distinguished from SWCNTs (constituted only of carbon atoms) by XPS and elemental analysis.

EXPERIMENTAL SECTION

Materials. Methyl methacrylate (MMA, Acros) was passed through a column of basic alumina prior to use and stored at −20 °C. Copper(I) bromide (Cu^IBr, Fluka) was purified via sequential washing with sulfurous acid, acetic acid, and ethanol, followed by drying under reduced pressure. Methyl 2-bromo-2-methylpropionate (MBMP, ≥99%, Aldrich), copper(II) bromide ($Cu^{II}Br$, ≥99%, Fluka), 2,2′-bipyridyl (bpy, ≥99%, Sigma-Aldrich), nickelocene ($NiCp_2$, 99%, Strem Chemicals), sodium iodide (NaI, ≥99%, Fluka), triphenylphosphine (PPh_3, ≥99%, Merck), and tetrahydrofuran (THF, anhydrous, ≥99.9%, Sigma-Aldrich) were used as received. Acetone (VWR) was purchased in the highest purity and used as received. *N*-Methylpyrrolidone (NMP, ≥98%, Fluka) was distilled under vacuum before use. The SWCNTs were purchased from He Ji Ltd. (diameter 1−2 nm, length 10−50 μm). SWCNTs were used as received with a content of SWCNTs up to 90 wt % and less than 1.5 wt % ashes (characteristics from the supplier). Dispersions of SWCNTs were filtered using a PTFE membrane (0.2 μm pore size, Sartorius).

Characterization. Thermogravimetric measurements were carried out on a Q5000 thermogravimetric analyzer from TA Instruments. Approximately 6 mg of sample was heated at 10 K min^{-1} from ambient temperature to 100 °C for 30 min and subsequently at the same heating rate from 100 to 700 °C in a dynamic air atmosphere (flow rate = 25 mL min^{-1}). Samples synthesized in NMP (see synthesis procedures **2a** and **2b**) were heated under the same conditions, except for the isothermal step conducted at 210 °C in order to evaporate potentially adsorbed NMP from the sample.

The elemental composition of the samples was analyzed using an automatic elemental analyzer Flash EA 1112 from Thermo Scientific, which was equipped with an MAS 200R autosampler. The calibration standards methionine, 2,5-bis-5-*tert*-butyl-2-benzoxazolylthiophene (BBOT), and vanadium pentoxide, tin capsules, and silver containers were purchased from IVA Analysentechnik e. K., Germany. Helium 5.0 for the GC-TCD analysis was purchased from Linde, Germany. A detailed description of the calibration of the equipment is provided in the Supporting Information.

XPS measurements were performed using a K-Alpha XPS spectrometer (ThermoFisher Scientific, East Grinstead, UK). Data acquisition

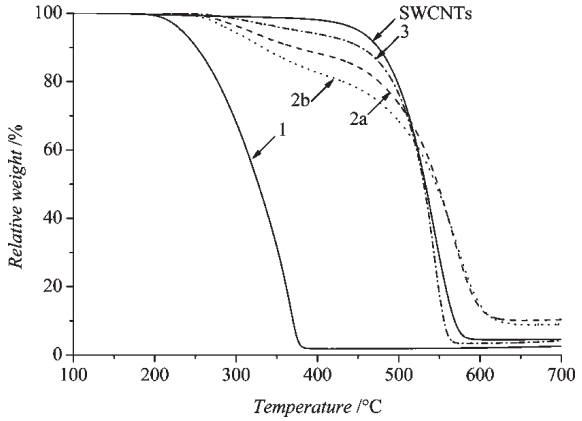

Figure 1. Thermogravimetric analysis in air atmosphere employing a heat flow of 10 °C min^{-1} of non-modified SWCNTs, (**1**) PMMA-Cp, (**2a**) SWCNTs modified with PMMA-Cp at ambient temperature, (**2b**) SWCNTs modified with PMMA-Cp at 80 °C, (**3**) blind sample (SWCNTs mixed with non-Diels−Alder reactive PMMA-Br at ambient temperature and subjected to the same washing procedure as **2a** and **2b**). Once the temperature reached 100 °C, the sample was equilibrated for 30 min at 100 °C for SWCNTs and **1**, as well as at 210 °C for **2a**, **2b**, and **3** to evaporate residual solvent (NMP).

and processing using the Thermo Avantage software is described elsewhere.[35] All SWCNTs were deposited on Au substrates and analyzed using a microfocused, monochromated Al Kα X-ray source (30−400 μm spot size). The K-Alpha charge compensation system was employed during analysis, using electrons of 8 eV energy and low-energy argon ions to prevent any localized charge buildup. The spectra were fitted with one or more Voigt profiles (BE uncertainty: ±0.2 eV). The analyzer transmission function, Scofield sensitivity factors,[36] and effective attenuation lengths (EALs) for photoelectrons[37] were applied for quantification. EALs were calculated using the standard TPP-2 M formalism. All spectra were referenced to the Au $4f_{7/2}$ peak at 84.0 eV binding energy controlled by means of the well-known photoelectron peaks of metallic Cu, Ag, and Au.

HRTEM analysis was performed with a Philips CM200FEG instrument, at 200 kV (large objective), the samples were prepared on copper grid with hollow polymer coverage.

Synthesis of Cyclopentadienyl-Capped Poly(methyl methacrylate) (PMMA-Cp, Sample 1). The synthesis of cyclopentadienyl-capped poly(methyl methacrylate) (PMMA-Cp) was performed according to the procedure described by Inglis et al.[34] The obtained intermediate polymer (PMAM-Br) and the cyclopentadienyl-capped polymer were characterized by size exclusion chromatography (SEC) and electrospray ionization mass spectrometry (ESI-MS) evidencing a molecular weight distribution of M_n = 2900 g mol^{-1} with a polydispersity index PDI = 1.2. The ESI-MS spectra confirm the successful and quantiative conversion from bromine to cyclopentadienyl-capped PMMA. A description of the experimental setup of the employed ESI-MS and the SEC system can be found in the Supporting Information (Figures S1−S3, Scheme S1, and Tables S1−S4) as well as a detailed characterization of the prepared polymers.

Synthesis of SWCNTs-Functionalized PMMA-Cp (Samples 2a and 2b). In a 100 mL round-bottom flask, 25 mg of SWCNTs were dispersed in 50 mL of distilled NMP in an ultrasonic bath. After 30 min of dispersion, 250 mg of PMMA-Cp (**1**) was added, and the mixture were stirred overnight at ambient temperature (**2a**). The dispersion was subsequently filtered and washed with 100 mL of THF and dried under vacuum. **2b** was synthesized under the same conditions, except that the dispersion was heated at 80 °C after the ultrasonic treatment. The round-bottom flask was capped with dried $CaCl_2$ to ensure no absorption of moisture. A blind sample (**3**) was prepared under exactly the same reaction conditions (including the washing procedure) as sample **2a** by replacing the PMMA-Cp polymer by its polymeric precursor PMMA-Br.

Table 1. Quantitative Grafting Results Obtained via TGA[a] of Non-modified SWCNTs: PMMA-Cp (1) and SWCNTs Modified with PMMA-Cp (2a)[b] and (2b)[c]

	T_i^e/°C	T_f^f/°C	T_{max}^g/°C	wt % at T_f
SWCNTs[d]	350	600	545	4.5
1	140	400	290	1.9
2a	200	410	325	87.7
	410	650	565	10.1
2b	200	410	325	81.8
	410	650	570	8.8
3	200	410	325	93.5
	410	600	545	4.5

[a] TGA conditions: air atmosphere, heat flow of 10 °C min^{-1}, after 30 min isothermal step at 100 °C for SWCNTs and **1**, and at 210 °C for **2a**, **2b**, and **3**. [b] At ambient temperature. [c] At 80 °C. [d] Non-modified SWCNTs. [e] Initial temperature for degradation. [f] Final temperature for degradation. [g] Temperature of maximal weight loss (from first derivative).

RESULTS AND DISCUSSION

As the reaction sequence is facile, the main task lies in the quantitative characterization of the grafted SWCNTs. Thermogravimetric analysis, elemental analysis, and X-ray photoelectron spectroscopy were conducted for the PMMA-Cp-modified SWCNTs (**2a**) and (**2b**) as well as for the non-modified SWCNTs and the initial polymer PMMA-Cp (**1**).

Thermogravimetric Analysis (TGA). The thermogravimetric analysis of the four samples and a blind reference in air atmosphere (see Figure 1) depicts noticeable differences between the nonmodified SWCNTs and the blind reference, on the one hand, and the PMMA-Cp modified SWCNTs **2a** and **2b**, on the other hand. Whereas non-modified SWCNTs remain stable until degradation commences at 350 °C, the PMMA-Cp modified SWCNTs start to degrade at lower temperature in two steps.

The analysis of the first derivative curves of the TGA traces for **2a** and **2b** indicates that initial degradation sets in at 210 °C with a maximal temperature (T_{max} for which the weight loss is maximal, see Supporting Information Figure S4) at 325 °C, while the subsequent degradation step has a similar maximal temperature T_{max} compared to non-modified SWCNTs (see Table 1).

Such a behavior is to be expected when a covalent attachment to the SWCNTs surface has indeed occurred: the tethered polymer strands on **2a** and **2b** should feature a similar degradation temperature as the pure polymer sample (PMMA-Cp). This is indeed observed (see Figure 1 and Figure S4 indicating identical maximal (T_{max}) and final (T_f) temperatures characteristic for the polymer degradation part). However, the overall degradation profile of **2a** and **2b** is indeed strongly altered when compared to the virgin SWCNTs (where *no* degradation is observed in the sub-350 °C region), providing evidence—underpinned by the below discussed blind sample degradation profile—for a successful functionalization of SWCNTs via a [4 + 2] cycloaddition with PMMA-Cp. The final temperature for

degradation (T_f) was determined graphically (see Supporting Information Figure S4) and represents the temperature at which the first degradation stops. Considering the weight loss at T_f, a further analysis of the obtained TGA curves allows the quantification of the amount of polymer chains grafted onto the surface of the SWCNTs. With observed weight percentages of 12.3% and 18.2% for **2a** and **2b**, respectively, the amount of polymer on the surface of the SWCNTs after washing is relatively high. Further underpinning these results, the thermogravimetric profile of the blind sample (**3**) displays a slight degradation, probably due to a small amount of PMMA-Br adsorbed at the surface of the SWCNTs. However, samples **2a** and **2b** display a much stronger degradation, unambiguously evidencing the covalent attachment of PMMA-Cp at the SWCNT's surface. The strongly altered thermal degradation profile observed in the profiles of the SWCNTs that have undergone a Diels−Alder reaction with PMMA-Cp, compared to the blind sample, provides a direct proof for not an adsorption of the polymer chains onto the surface of the SWCNTs, but rather a covalent functionalization.

For a better understanding and comparison of the grafting density onto nanoparticles, these experimental values must be expressed in commonly used units for the grafting density. Moreover, a mathematical treatment must take into account the amount of impurities, the molecular weight of the polymer chains, and the specific surface area of the graphene sheet (details explained in the Supporting Information, eqs S1−S3). The periodicity represents the surface occupied by the polymer chains for the specific application of grafting CNTs. Expressed by the number of carbon atoms covered by a single polymer chain, this value subsequently allows for a qualitative analysis with reference to the structure of the SWCNTs. According to Table 4 (see below, where all quantitative grafting data from all three methods are compiled), a higher grafting ratio results for the sample reacted at 80 °C (**2b**) compared with that of the sample reacted at ambient temperature (**2a**), with 0.040 and 0.025 chains nm^{-2}, respectively. A maximum theoretical grafting density can be calculated, assuming that every unsaturated carbon double bond reacts with a polymer chain. This means that the periodicity is reduced by one polymer chain every two carbon atoms of the SWCNTs, leading to grafting density of 41.62 mmol g^{-1} or 19 chains nm^{-2} with an estimated specific surface of the SWCNTs (or graphene sheet) of 1315 m^2 g^{-1} [38] (see Supporting Information eqs S5 and S6 for calculation details). These theoretical values are, however, very unrealistic and do not take into account the steric demand of a polymer chain after the reaction onto the SWCNTs surface. Using an ideal polymer chain model, i.e., the equivalent of an attached chain that occupies space on the surface[39] for PMMA-Cp, calculation leads to a theoretical radius of gyration $\langle R_g \rangle$ of 1.66 nm, which can be exploited to deliver more reasonable theoretical grafting densities (see Supporting Information eqs S7−S9 for calculation details). The corresponding disk is then defined with a square radius of $2\langle R_g \rangle^2$. From this theoretical disk (radius of 2.35 nm), the grafting density of the polymer can be calculated for the corresponding surface of the SWCNTs. Thus, the theoretical grafting ratio can be expressed as one polymer chain every 659 carbon atoms (0.126 mmol g^{-1} or 0.058 chains nm^{-2}) which is not far removed from the experimentally found values for the two samples studied (50% (**2a**) and 67% (**2b**) of the theoretical grafting density). The somewhat smaller grafting density obtained experimentally may be explained by the presence of SWCNT bundles not completely dispersed after ultrasonic dispersion before the functionalization with the polymer.

Table 2. Elemental Analysis Results of Nonmodified SWCNTs, PMMA-Cp (1), and SWCNTs Modified with PMMA-Cp (2a)[a] and (2b)[b]

	wt %[d]			
	C	H	N	O
SWCNTs[c]	85.4	1.7	0.8	2.2
1	58.3	7.7	1.0	30.2
2a	74.6	1.8	1.8	7.0
2b	73.6	1.9	2.2	7.7

[a] At ambient temperature. [b] At 80 °C. [c] Nonmodified SWCNTs. [d] Number of carbon atoms covered by one polymer chain grafted on the surface of SWCNTs.

Elemental Analysis (EA). In order to confirm the grafting density observed by TGA, elemental analysis was performed on all the samples. With high accuracy, the results for PMMA-Cp are in excellent agreement with the stoichiometry of the polymer (see Table 2). The presence of other elements for non-modified SWCNTs reveals the presence of adsorbed molecules from the air and some impurities in the sample. Measurements of the sulfur content were performed, yet this element was not detected, since it is not involved in the synthetic procedure. The content of hydrogen for the carbon nanotube-based samples (SWCNTs, **2a**, and **2b**) is very low. For this reason, the elemental analysis leads to slight fluctuations in the carbon and oxygen content. Nevertheless, one can observe a significant presence of oxygen content in the functionalized SWCNTs. As explained in detail in the Supporting Information eqs S1−S4, the grafting ratio of polymer on the SWCNTs can be estimated from the ratio between carbon and oxygen atoms. The grafting density in wt % for the SWCNTs modified with PMMA-Cp at ambient temperature (**2a**) was calculated to be 19.2% and at 80 °C (**2b**) 22.1% (see Table 4, see below, where all quantitative grafting data from all three methods are compiled). Close inspection of the numbers collected in Table 2 reveals two facts: (*i*) the order of magnitude for the grafting ratios is similar to those obtained via TGA, and (*ii*) the same trends are observed with regard to the reaction conditions (0.025 chains nm^{-2} (TGA) vs 0.038 chains nm^{-2} (EA) for ambient temperature and 0.040 chains nm^{-2} (TGA) vs 0.045 chains nm^{-2} (EA) for sample reacted at 80 °C).

X-ray Photoelectron Spectroscopy (XPS). Further investigations with XPS (see Figure 2) provide information about the elemental composition and chemical binding states of the samples in a non-destructive manner. The presence of O 1s peak components attributed to PMMA-Cp directly proves the successful functionalization of the SWCNTs. The XPS quantification together with the binding energy assignments are compiled in Table 3. For more clarity, the detailed C 1s spectra for each sample are reported in the Supporting Information (Figure S5).

Non-modified SWCNTs as well as PMMA-Cp (**1**) were measured as reference samples in order to facilitate the interpretation of the XPS spectra obtained for the PMMA-Cp modified SWCNTs (**2a** and **2b**). The C 1s binding energy at 284.4 eV, as well as the peak shape found for the SWCNTs, is in a good agreement with the literature[40,41] and is therefore used as a template to fit the C 1s spectra of the PMMA-Cp-modified SWCNTs samples **2a** and **2b**. Additionally, the $\pi-\pi^*$ transition,

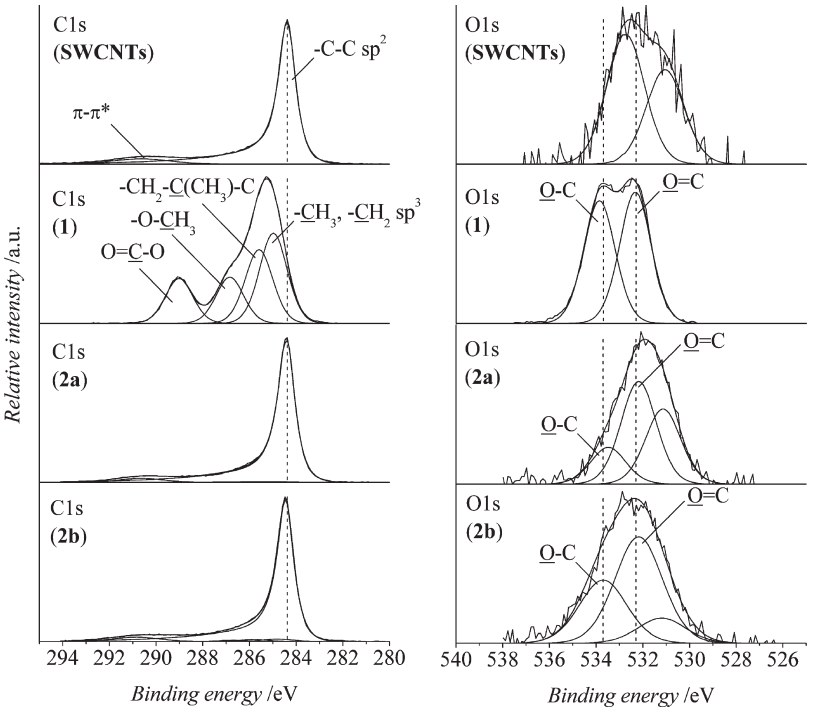

Figure 2. XPS spectra of non-modified SWCNTs, (**1**) PMMA-Cp, (**2a**) SWCNTs modified with PMMA-Cp at ambient temperature, and (**2b**) SWCNTs modified with PMMA-Cp at 80 °C. The C 1s signal from modified SWCNTs (C−C sp^2 at 284.4 eV) is represented. The O 1s peaks at 532.3 eV (−O−C═O) and 533.7 eV (−O−CH_3) are attributed to PMMA and indicate the successful functionalization in **2a** and **2b**. The peak at 531.1 eV is probably due to surface contamination or reaction residuals (observable at 531.1 and 532.8 eV from SWCNTs).

Table 3. Assignments of binding energy and comparison of atomic bond contribution after the deconvolution of the XPS spectra of non-modified SWCNTs, PMMA-Cp (1), and SWCNTs Modified with PMMA-Cp (2a)[a] and (2b)[b]

		at. %				
atom	BE/eV	SWCNTs[c]	**1**	**2a**	**2b**	entity
C 1s	284.4	85.9		83.8	80.2	C−C sp^2
	285.0		25.8	0.6	1.8	−CH_2, −CH_3 sp^3
	285.7		21.1	0.5	1.4	−CH_2−C(CH_3)−$COOCH_3$
	286.8		13.2	0.3	0.9	−OCH_3
	289.1		12.8	0.3	0.9	O═C−OCH_3
	290.7	7.1		3.9	4.7	π−π*
O 1s	532.3		13.7	2.2	2.6	O═C−OCH_3
	533.7		12.8	0.8	1.5	OCH_3

[a] At ambient temperature. [b] At 80 °C. [c] Nonmodified SWCNTs. The C 1s peak at 531.1 eV for the PMMA-modified samples (**2a** with 1.6 at. % and **2b** with 0.6 at. %) is probably due to surface contamination (observable at 531.1 and 532.8 eV from SWCNTs, respectively 0.6 and 0.9 at. %).

well-known for graphitic and aromatic compounds (sp^2 hybridization), is found at 290.7 eV. A negligible amount of contamination is indicated by weak O 1s components (peaks at 531.1 and 532.8 eV, respectively 0.6 and 0.9 at. %) and is due to atmospheric contact of the samples prior to the XPS measurements.

In the case of PMMA-Cp (**1**), the C 1s spectrum shows four components consistent with the known structure of PMMA. Aliphatic carbon (−CH_2, −CH_3) with a C 1s signal at 285.0 eV, quaternary carbon (−CH_2−C(CH_3)−$COOCH_3$) at 285.8 eV, methoxylic carbon (−OCH_3) at 286,8 eV, and carboxylic carbon (O═C−OCH_3, 289.1 eV) were identified. The corresponding O 1s components were measured at 532.3 eV (O═C−OCH_3) and 533.1 eV (−OCH_3). The binding energies as well as the stoichiometry correspond excellently with former measurements performed on PMMA.[42]

Considering these results, the deconvolution of the spectra of the modified SWCNTs samples **2a** and **2b** evidence that the reaction with PMMA-Cp through the formation of the norbornene entity at the surface of the SWCNTs occurred. However, the differentiation of C−C peaks from aliphatic carbons (primary, secondary, and quaternary) of the polymer backbone remains difficult, since the tail of the SWCNT component dominates the high-energy shape of the C 1s multiplet (see Figure 2). Consequently, the quantitative contribution of each identified entity cannot be employed to determine the grafting density. In contrast, the O 1s peaks (532.3 and 533.7 eV) indicate directly the uptake of PMMA-Cp as the respective O 1s components are not detectable in the spectra of non-modified SWCNTs. However, compared to the PMMA-Cp reference data, the intensity of the carboxylic component (peaks at 531.1 eV) for the PMMA-Cp-modified SWCNTs samples **2a** and **2b** is higher and is probably due to atmospheric contamination as already observed for the non-modified SWCNTs.

The atomic amount of oxygen atoms estimated for the modified SWCNTs **2a** and **2b** (3 and 4.1 at. %, respectively) is sufficiently significant to conclude a successful functionalization of the SWCNTs with the polymer PMMA-Cp and to calculate the grafting density of the samples (see Table 4). Based on the same consideration as for TGA measurements with the specific area of the SWCNTs, the grafting ratio was calculated according to the increase of oxygen content of the modified SWCNTs

Table 4. Grafting Ratios of PMMA-Cp Functional SWCNTs 2a[a] and 2b[b] Based on TGA, EA, and XPS Results for C and O Atomic Content[c]

		grafting ratio			
		wt % of polymer	mmol g^{-1}	chains nm^{-2}	periodicity[d]
2a	TGA	12.3	0.055	0.025	1523
	EA	19.2	0.082	0.038	1015
	XPS	13.0	0.052	0.024	1615
	average	14.8	0.064	0.029	1384
2b	TGA	18.2	0.086	0.040	968
	EA	22.1	0.098	0.045	850
	XPS	17.9	0.075	0.034	1108
	average	19.4	0.086	0.039	975

[a] At ambient temperature. [b] At 80 °C. [c] The calculation proceeded by considering the reference (nonmodified SWCNTs), the polymer (PMMA-Cp), and the theoretical graphene sheet specific surface area (1315 g m^{-2}). A detailed sample calculation can be found in the Supporting Information. [d] Number of carbon atoms covered by one polymer chain grafted on the surface of SWCNTs.

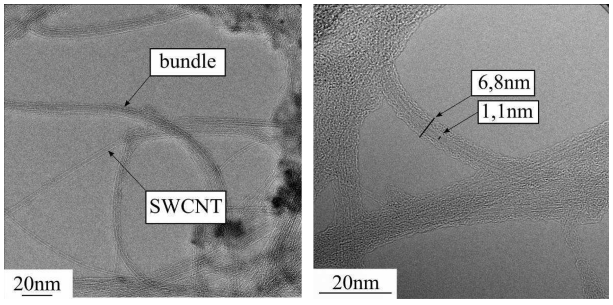

Figure 3. HRTEM pictures of nonmodified SWCNTs (left) and (**2b**) SWCNTs modified with PMMA-Cp at 80 °C (right).

compared to the non-modified ones (see Supporting Information eqs S1−S3). Pleasingly, the same order of magnitude for the grafting ratios observed by XPS as for TGA and EA measurements evidence a successful functionalization of SWCNTs with cyclopentadienyl end-capped poly(methyl methacrylate) through [4 + 2] Diels−Alder cycloaddition.

To allow for a better comparability of all results, Table 4 summarizes the grafting ratios and densities obtained by the three independent techniques as well as providing average values. However, as discussed above, the quantitative grafting ratios obtained via XPS appears to be the most reliable.

High-Resolution Transmission Electron Microscopy (HRTEM). In order to further support the above quantitative results of the described chemical and physical analysis, HRTEM was performed on the modified and nonmodified samples. The HRTEM observations of the functionalized SWCNTs (see Figure 3) reveals the presence of a ∼3 nm thick uniform surrounding layer on the surface of the SWCNTs with a diameter of 1 nm, whereas no comparable structure was observed for the non-modified SWCNTs, further macroscopically underpinning the functionalization of SWCNTs with PMMA-Cp evidenced by the above quantitative methods. HRTEM observations enable also to justify the comparison of XPS quantification with the results observed by elemental analysis, since an overall 6.8 nm diameter for the covalently modified SWCNTs is observed and corresponds to the XPS sampling depth of 5−10 nm. From the theoretical value obtained by approximating the polymer chain with a disk of radius 2.35 nm, it can be postulated that the polymer chains wrap the cylindrical surface of the SWNCTs and do not stand as rods at the surface.

CONCLUSIONS

The [4 + 2] cycloaddition of cyclopentadienyl end-capped poly(methyl methacrylate) to single-walled carbon nanotubes was performed under mild conditions, without catalyst and at ambient temperature as well as at 80 °C. The facile access to well-defined and quantitatively cyclopentadienyl-capped macromolecules via an efficient −Br to cyclopentadiene switch makes the method especially appealing. The grafting reaction was quantitatively evidenced by macroscopic measurements (TGA, EA) with spectroscopic tools (XPS) and observed at the nanoscopic scale (HRTEM). The [4 + 2] reaction for functionalizing the carbon nanotubes occurred in a single step, opening a facile and innovative strategy for modifying carbon nanotubes for their subsequent use in polymeric nanocomposites, thus significantly simplifying the engineering of such materials.

ASSOCIATED CONTENT

Supporting Information. Description of the calibration for EA, the description of the experimental setup for the ESI-MS and the employed SEC system (Figures S1−S3, Scheme S1, and Tables S1−S4), the first derivative analysis of the TGA profiles (Figure S4), the calculation details of the grafting density from the TGA measurements (eqs S1−S3), EA measurements (eq S4) as well as from the XPS measurement (Figure S5) and the calculation of the grafting density, the theoretical grafting density at the SWCNT's surface for completely functionalized SWCNTs (eqs S5 and S6) and by considering an ideal chain (eqs S7−S9). This material is available free of charge via the Internet at http://pubs.acs.org.

AUTHOR INFORMATION

Corresponding Author

*Tel +49 721 608 45641, Fax +49 721 608 45740, e-mail christopher.barner-kowollik@kit.edu.

ACKNOWLEDGMENT

C.B.-K. acknowledges funding for the current project from the Fraunhofer Institute for Chemical Technology (ICT). In addition, funding in the context of the Excellence Initiative for leading German universities, the German Research Council (DFG) as well as the Ministry of Science and Arts of the State of Baden-Württemberg, is gratefully acknowledged. The authors are additionally thankful to Dr. Detlef Schmiedl (ICT Fraunhofer) for carrying out the elemental analysis experiments as well as to Dr. Frank Hennrich (KIT, Institute for Nanotechnology) for his helpful advice.

REFERENCES

(1) Spitalsky, Z.; Tasis, D.; Papagelis, K.; Galiotis, C. *Prog. Polym. Sci.* **2010**, *35*, 357–401.

(2) Yang, B.-X.; Shi, J.-H.; Pramoda, K. P.; Goh, S. H. *Nanotechnology* **2007**, *18*, 125606–125612.

(3) Blake, R.; Coleman, J. N.; Byrne, M. T.; McCarthy, J. E.; Perova, T. S.; Blau, W. J.; Nagy, J. B.; Gun'ko, Y. K. *J. Mater.Chem.* **2006**, *16*, 4206–4213.
(4) Bauhofer, W.; Kovacs, J. Z. *Compos. Sci. Technol.* **2008**, *69*, 1486–1511.
(5) Huang, Y. Y.; Terentjev, E. M. *Adv. Funct. Mater.* **2010**, *23*, 4062–4068.
(6) Bose, S.; Bhattacharyya, A. R.; Kulkarni, A. R.; Pötschke, P. *Compos. Sci. Technol.* **2009**, *69*, 365–372.
(7) Fujigaya, T.; Fukumaru, T.; Nakashima, N. *Synth. Met.* **2009**, *159*, 827–830.
(8) Li, X.; Gao, H.; Scrivens, W. A.; Fei, D.; Xu, X.; Sutton, M. A.; Reynolds, A. P.; Myrick, M. L. *J. Nanosci. Nanotechnol.* **2007**, *7*, 2309–2317.
(9) Kashiwagi, T.; Fagan, J.; Douglas, J. F.; Yamamoto, K.; Heckert, A. N.; Leigh, S. D.; Obrzut, J.; Du, F.; Lin-Gibson, S.; Mu, M.; Winey, K. I.; Haggenmueller, R. *Polymer* **2007**, *48*, 4855–4866.
(10) Uchida, T.; Kumar, S. *J. Appl. Polym. Sci.* **2005**, *98*, 985–989.
(11) Hirsch, A.; Votroswsky, O. *Top. Curr. Chem.* **2005**, *245*, 193–237.
(12) Banerjee, S.; Hemraj-Benny, T.; Wong, S. S. *Adv. Mater.* **2005**, *1*, 17–29.
(13) Peng, X.; Wong, S. S. *Adv. Mater.* **2009**, *21*, 625–642.
(14) Tchoul, M. N.; Ford, W. T.; Lolli, G.; Resasco, D. E.; Arepalli, S. *Chem. Mater.* **2007**, *19*, 5765–5772.
(15) Datsyuk, V.; Kalyva, M.; Papagelis, K.; Parthenios, J.; Tasis, D.; Siokou, A.; Kallitsis, I.; Galiotis, C. *Carbon* **2008**, *46*, 833–840.
(16) Touhara, H.; Inahara, J.; Mizuno, T.; Yokoyama, Y.; Okanoa, S.; Yaganiuch, K.; Mukopadhyay, I.; Kawasaki, S.; Okino., F.; Shirai, H.; Xu, W. H.; Kyotani, T.; Tomita, A. *J. Fluorine Chem.* **2002**, *114*, 181–188.
(17) Ying, Y.; Saini, R. K.; Liang, F.; Sadana, A. K.; Billups, W. E. *Org. Lett.* **2003**, *5*, 1471–1473.
(18) Holzinger, M.; Votrowski, O.; Hirsch, A.; Hennrich, F.; Kappes, M.; Weiss, R.; Jellen, F. *Angew. Chem.* **2001**, *40*, 4002–4005.
(19) Brunetti, F.; Ferrrero, M.; Munoz, J.; Meneghetti, M.; Prato, M.; Vasquez, E. *J. Am. Chem. Soc.* **2008**, *130*, 8094–8100.
(20) Coleman, K. S.; Bailey, S. R.; Fogden, S.; Green, M. L. H. *J. Am. Chem. Soc.* **2003**, *125*, 8722–8723.
(21) Gebhardt, B.; Graupner, R.; Hauke, F.; Hirsch, A. *Eur. J. Org. Chem.* **2010**, *8*, 1494–1501.
(22) Martinez-Rubi, Y.; Guan, J.; Lin, S.; Scriver, C.; Sturgeon, R. E.; Simard, B. *Chem. Commun.* **2007**, *48*, 5146–5148.
(23) Barner-Kowollik, C.; Du Prez, F. E.; Espeel, P.; Hawker, C. J.; Junkers, T.; Schlaad, H.; van Camp, W. *Angew. Chem., Int. Ed.* **2011**, *50*, 60–62.
(24) Nebhani, L.; Barner-Kowollik, C. *Macromol. Rapid Commun.* **2010**, *31*, 1298–1305.
(25) Giacalone, F.; Martin, N. *Chem. Rev.* **2006**, *106*, 5136–5190.
(26) Kymakis, E.; Servati, P.; Tzanetakis, P.; Koudoumas, E.; Kornolios, N.; Rompogiannakis, I.; Franghiadakis, Y.; Amaratunga, G. A. J. *Nanotechnology* **2007**, *18*, 435702–435705.
(27) Lu, X.; Tian, F.; Wang, N.; Zhang, Q. *Org. Lett.* **2002**, *24*, 4313–4315.
(28) Mercuri, F.; Sgamellotti, A. *Phys. Chem. Chem. Phys.* **2009**, *11*, 563–567.
(29) Nunzi, F.; Smagellotti, A.; De Angelis, F. *Chem.—Eur. J.* **2009**, *15*, 4182–4189.
(30) Ménard-Moyon, C.; Dumas, E.; Doris, F.; Mioskowski, C. *J. Am. Chem. Soc.* **2006**, *128*, 14764–14765.
(31) Munirasu, S.; Albuerne, J.; Boschetti-de-Fierro, A.; Abetz, V. *Macromol. Rapid Commun.* **2010**, *31*, 574–579.
(32) Sakellariou, G.; Ji, H.; Mays, J. W.; Hadjichristidis, N.; Baskaran, D. *Chem. Mater.* **2007**, *19*, 6370–6372.
(33) (a) Gruendling, T.; Weidner, S.; Falkenhagen, J.; Barner-Kowollik, C. *Polym. Chem.* **2010**, *1*, 599–617. (b) Advoshenko, S. M.; Ioffe, I. N.; Kozlov, A. A.; Markov, V. Y.; Nikolaev, E. N.; Sidorov, L. N. *Rapid Commun. Mass Spectrom.* **2008**, *22*, 1372–1376.
(34) Inglis, A. J.; Paulöhrl, T.; Barner-Kowollik, C. *Macromolecules* **2010**, *43*, 33–36.
(35) Parry, K. L.; Shard, A. G.; Short, R. D.; White, R. G.; Whittle, J. D.; Wright, A. *Surf. Interface Anal.* **2006**, *38*, 1497–1504.
(36) Scofield, J. H. *J. Electron Spectrosc. Relat. Phenom.* **1976**, *8*, 129–148.
(37) Tanuma, S.; Powell, C. J.; Penn, D. R. *Surf. Interface Anal.* **1994**, *21*, 165–176.
(38) Peigney, A.; Laurent, C.; Flahaut, E.; Bacsa, R. R.; Rousset, A. *Carbon* **2001**, *39*, 507–514.
(39) Rubinstein, M.; Colby, R. In *Polymer Physics*; Rubinstein, M., Colby, R., Eds.; Oxford University Press: New York, 2001; pp 40−70.
(40) Retzko, I.; Unger, W. E. S. *Adv. Eng. Mater.* **2003**, *5*, 519–522.
(41) Pumera, M.; Smid, B.; Veltruska, K. *J. Nanosci. Nanotechnol.* **2009**, *9*, 2671–2676.
(42) De Marco, C.; Eaton, S. M.; Suriano, R.; Turri, S.; Levo, M.; Rampino, R.; Cerullo, G.; Osellame, R. *ACS Appl. Mater. Interfaces* **2010**, *2*, 2377–2384.